Approach for maximizing chaotic mixing in microfluidic devices

Sanjeeva Balasuriya[a)]
School of Mathematics and Statistics, University of Sydney, New South Wales 2006, Australia

(Received 21 November 2004; accepted 4 August 2005; published online 14 November 2005)

This paper uses recent theoretical work to determine the best configurations for cross-channel micromixers in optimizing mixing between two fluids. Insight into the positioning, widths, and flow protocols within the lateral channels is provided. © *2005 American Institute of Physics*.
[DOI: 10.1063/1.2042507]

Microfluidic devices (in which dimensions are typically of the order of millimeters, and which handle fluid volumes of the order of nanoliters) have seen a recent explosion of interest, with significant potential applications in drug delivery and monitoring, cell culture, gene profiling, chemical synthesis, "lab-on-a-chip" printing, and protein analysis.[1–6] The inevitable low Reynolds number limit in such devices means that turbulent mixing is suppressed. Diffusion by itself is not sufficiently effective in obtaining well-mixed solutions in some applications, leading to an interest in deterministic chaos as a mixing mechanism [see also the entire issue of [7–16] Philos. Trans. R. Soc. London, Ser. A **362**, 923 (2004)].

A variety of diagnostics are frequently used as measures of mixing, such as Lyapunov exponents, effective diffusivities, transition or escape rates, etc. (see, for example, Refs. 15–21). Nevertheless, these often provide little insight into the best mixing protocols that enhance mixing, resulting in very few available investigations on mixing optimization.[12,13,20,22] Recent theoretical work,[22,23] which utilizes lobe dynamics and Melnikov techniques[24,25] to precisely quantify flux across flow separatrices, provides a method to do so. This is particularly relevant to cross-channel micromixers,[7–10] a schematic illustration of which is presented in Fig. 1. Fluids A and B, entering the micromixer from two sides, tend not to mix across the dashed line, which acts as a flow separatrix. How and where should perturbing fluid channels be placed to maximize mixing?

A brief description of the theoretical basis upon which this question is to be answered will be first presented. Any perturbed flow expressible as

$$\dot{x} = -\frac{\partial H}{\partial y} + \varepsilon g_1(x,y)\cos(\omega t - \beta),$$
$$\dot{y} = \frac{\partial H}{\partial x} + \varepsilon g_2(x,y)\cos(\omega t - \beta), \tag{1}$$

is amenable to this analysis. Here $H(x,y)$ is the Hamiltonian for the unmixed incompressible flow (such as that in Fig. 1), and $0 < \varepsilon \ll 1$. The perturbing term $\mathbf{g} = (g_1, g_2)$ is to be chosen to optimize mixing. The $\varepsilon = 0$ flow must possess a trajectory Γ that connects two hyperbolic stagnation points; it is across this that chaotic flux is to be assessed. Suppose Γ is given by the heteroclinic trajectory $(\bar{x}(t), \bar{y}(t))$, thereby providing a parametrization for Γ with $t \in \mathbb{R}$. By determining leading-order perturbations of this separatrix using a Melnikov analysis,[25,26] computing the area of the lobes created,[24,25] and then rationalizing the chaotic flux *directly* as a volume of fluid transferred per unit time,[22,23,27] it is possible to express directly the chaotic flux across Γ as a perturbative expansion $\varepsilon\, s(\omega) + \mathcal{O}(\varepsilon^2)$ in which

$$s(\omega) = \sqrt{\frac{2}{\pi}} \left| \mathcal{F}\{\nabla H \cdot \mathbf{g}(\bar{x}(t), \bar{y}(t))\}(\omega) \right|, \tag{2}$$

where $\mathcal{F}$ is the standard Fourier transform (see Refs. 22 and 23). For a given $\mathbf{g}$, Eq. (2) is a computationally powerful method for determining the flux for a given perturbation and frequency, particularly so given the prevalence of Fourier transform software.

Given a frequency ω, how can one choose $\mathbf{g}$ subject to a given maximum bound $|\mathbf{g}(x,y)| \leq G$, in order to maximize the flux? Choosing $\mathbf{g}$ parallel to ∇H is incorrect, because of the phase of $\mathcal{F}$ in Eq. (2). There is, however, a time shift $\psi(\omega, \beta)$ that can be applied to the heteroclinic trajectory $(\bar{x}(t), \bar{y}(t))$ that makes $\mathcal{F}$ purely real; this is since a t shift is equivalent to a rotation in Fourier space, and has no effect on the modulus in Eq. (2). Once this shift has been applied, optimizing Eq. (2) simply requires choosing $\mathbf{g}$ on Γ to be as close as possible to the *unphysical* perturbation

$$\mathbf{g_m}(\ell) = G\, \mathrm{sign}\{\cos[\omega t(\ell)]\} \frac{\nabla H(\ell)}{|\nabla H(\ell)|}, \tag{3}$$

where ℓ is the arclength parametrization along Γ, whose monotonic relationship with t is given by

$$\ell(t) = \int_{-\infty}^{t} |\nabla H(\bar{x}(\tau), \bar{y}(\tau))|\, d\tau, \tag{4}$$

with $t(\ell)$ being its inverse. The sign flipping is necessary to ensure that the cosine terms always contribute positively towards the flux. This represents infinitely many streams of constant speed G flowing perpendicularly across Γ such that adjacent streams are exactly out of phase with one another. Intuitively, this strange form for $\mathbf{g}_m$ works because the perturbed stable and unstable manifolds intersect infinitely often along Γ, at points that are π/ω apart in t. A particular manifold needs to be pushed in *different* directions in each of

a)Electronic mail: sanjeeva@maths.usyd.edu.au

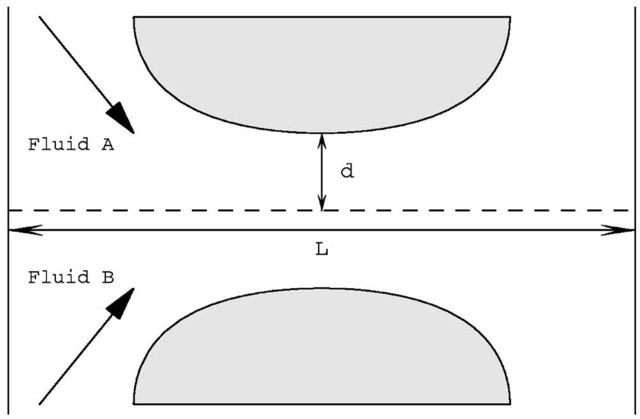

FIG. 1. A microdevice as a basis for a cross-channel micromixer.

these alternating segments in order to make the intersecting lobes bigger, thereby increasing the chaotic region.

For any perturbation $\mathbf{g}$, the flux $s(\omega) < s_m(\omega)$, where $s_m(\omega)$ is the flux corresponding to g_m, given by[22]

$$s_m(\omega) = \frac{G}{\pi} \sup_{\psi \in \left[0, \frac{\pi}{\omega}\right)} \int_{-\infty}^{\infty} \left| \nabla H(\bar{x}(t), \bar{y}(t)) \cos[\omega(t+\psi)] \right| dt. \tag{5}$$

In the above, "sup" indicates the maximum value. The proper choice of ψ is the phase used to make the Fourier transform real, and taking the maximum compensates for the lack of knowledge of this phase shift. See Ref. 22 for more detail on the structure of $s_m(\omega)$.

The focus here is to apply these ideas to cross-channel micromixers to determine the optimal design strategy. Given a particular base flow geometry and speed, begin by choosing an appropriate Hamiltonian function. One that works for Fig. 1 is $H(x,y) = -a \sin(\pi x/L) \sin(\pi y/L)$ (where $a, L > 0$), an Euler solution familiar from a variety of contexts.[23,28–32] Here, the flow separator connects $(x,y) = (0,0)$ to $(0,L)$, and the top and bottom boundaries can themselves be expressed as $H(x,y) = \pm a \sin(\pi d/L)$, where $d = L/5$ in this figure. Modifying the computations in Refs. 22, 23, 29, and 30, it can be shown that $|\nabla H(\bar{x}(t), \bar{y}(t))| = (a\pi/L) \operatorname{sech}(a\pi^2 t/L^2)$ for the symmetric choice of time zero, and $\ell(t) = (2L/\pi) \tan^{-1}[\exp(a\pi^2 t/L^2)]$. For perturbations of the form (1), the leading-order term $s(\omega)$ of the flux is therefore bounded by

$$s_m(\omega) = \frac{Ga}{L} \sup_{\psi \in \left[0, \frac{\pi}{\omega}\right)} \int_{-\infty}^{\infty} \operatorname{sech}\left(\frac{a\pi^2 t}{L^2} \right) \left| \cos[\omega(t+\psi)] \right| dt. \tag{6}$$

Since the sech function is even and unimodal, the correct choice to maximize the effect of the cosine term above is $\psi = 0$ (independent of ω). A numerically computed graph of s_m appears as the heavy curve in Fig. 2. Also illustrated in this graph are curves resulting from incorrect choices in Eq. (6): $\psi = \pi/(4\omega)$ (dashed curve) and $\psi = \pi/(2\omega)$ (dotted curve). Such choices correspond to constant shifts in the time parametrization along Γ, or equivalently, constant t shifts applied to $\mathbf{g}_m[\ell(t)]$.

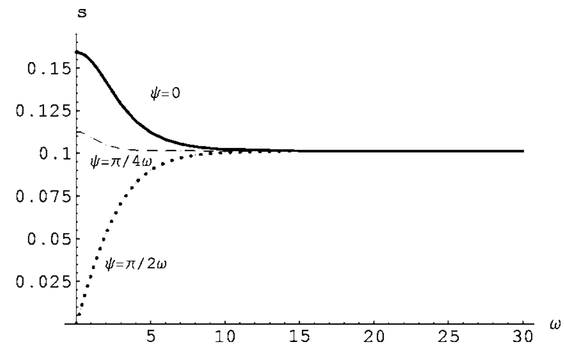

FIG. 2. Graph of s_m ($\psi = 0$) with $G = 1$, $a = 1/(2\pi)$, $L = 1/2$ (several incorrect choices of ψ are also shown).

For maximum flux s_m, the lateral channels need to change directions at

$$x_n = \frac{2L}{\pi} \tan^{-1}\left[\exp\left(\frac{a\pi^3(2n-1)}{2\omega L^2} \right) \right], \quad n \text{ an integer}, \tag{7}$$

resulting in channels whose widths differ from one another. Identify the jth channel as having endpoints x_j and x_{j+1}, with width $W_j = x_{j+1} - x_j$, whose variation with ω is shown in Fig. 3. The middle channel $(j=0)$ is wider than $j = \pm 1$, which is wider than $j = \pm 2$, etc. Differences are more pronounced for small frequencies, with channels approaching uniformity for large ω.

An illustration of how to set up these channels in the micromixer of Fig. 1, keeping in this case only the middle five of the infinitely many lateral channels that the theory describes, is presented in Fig. 4. This figure is *exactly* computed and to scale, with the choice $\omega = 50$, $d = 0.1$ and $L = 0.5$. The channel numbering is also shown. The arrows towards the bottom of the figure indicate that the lateral channel flow is to be exactly out of phase in adjacent channels. This perturbing flow can be set up through the time-harmonic variation of (i) imposed pressure gradient, (ii) pumping of Fluid A (from the top) and Fluid B (from the bottom), or (iii) vibration of horizontal walls in reservoirs just above and below the picture. The resulting fluid emerging from the right outlets of the apparatus is as well mixed as possible with respect to perturbations satisfying $|\mathbf{g}| \leq G$.

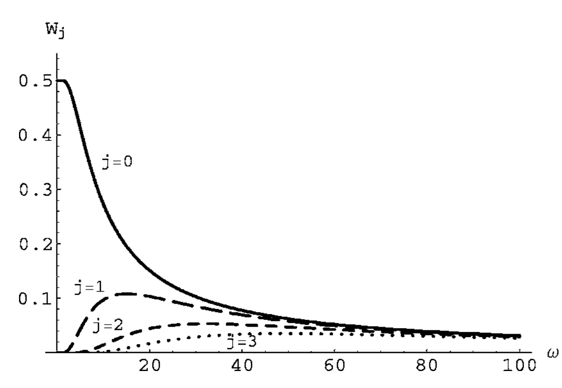

FIG. 3. Lateral channel length scale variation with frequency, with $G = 1$, $a = 1/(2\pi)$, and $L = 1/2$.

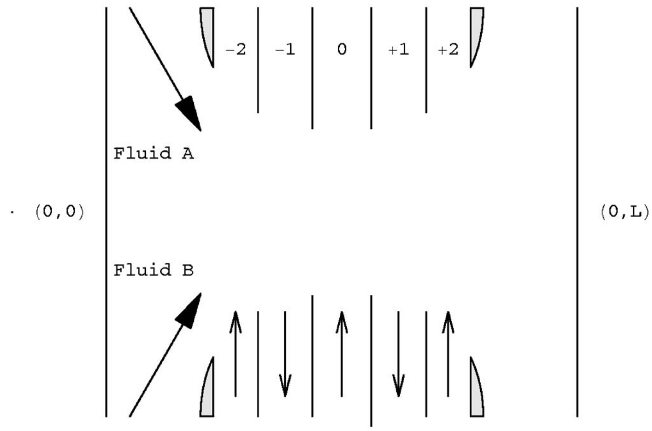

FIG. 4. An exact, to scale, diagram of the cross-channel micromixer with $\omega=50$, $d=0.1$, $L=0.5$, and five channels.

Fitting in more channels in Fig. 4 requires a smaller choice of d, effectively using streamlines closer to Γ as top/bottom boundaries. Indeed, the maximum number of channels N that is possible is given by

$$N < \frac{2\omega L^2}{a\pi^3}\ln\left[\cot\left(\frac{d\pi}{2L}\right)\right], \quad (8)$$

which is linear in the frequency, and inversely proportional to the flow speed parameter a. To quantify this inevitability of a *finite* number of lateral channels, define the mixing quality factor Q by s/s_m, where the flux s is computed either from Eq. (2) or by integrating over the suitable finite domain in Eq. (6). Figure 5 shows the quality factor as a function of the number of lateral channels (always chosen to be an odd number for symmetry) when $\omega=50$, and assuming that d is chosen such that this number of channels can be fitted in. The stars correspond to choosing the optimum channel structure similar to Fig. 4. In order to address more familiar micromixer arrangements that have separated lateral channels,[7–10] the diamonds give the result of using only the *even*-indexed channels. In this instance, the fluids in all the channels oscillate in phase with one another. The quality factor is considerably worse than in the previous case. It may be thought that having such (even-indexed) channels oscillating *out of phase* with adjacent channels (channels ±2, ±6, ±10, etc, being out of phase with channels 0, ±4, ±8, etc.) may produce greater mixing. The triangles in

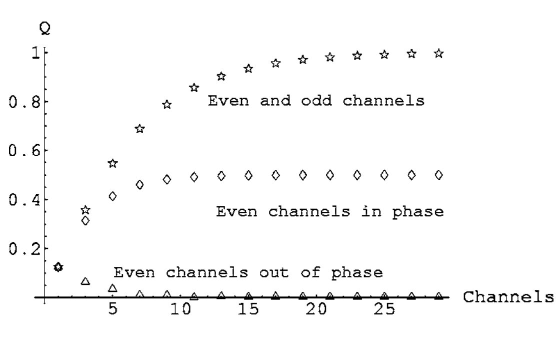

FIG. 5. Mixing quality factor as a function of the number of lateral channels when $\omega=50$.

Fig. 5 show that this is not the case, and even more disturbingly, the quality factor decreases with increasing channels. While the positioning of these channels in this instance is contrived (it is the "worst" lateral forcing to use, which pushes manifolds together), this should be thought of as a caution—the positioning and the directions of motion along the lateral channels needs to be carefully managed to optimize mixing. For example, using channels $-5, -2, +1, +4, +7$, etc., with adjacent channels being exactly out of phase, is flux enhancing.

There are clearly many practical difficulties in designing micromixers as outlined here. Infinitely many lateral channels (eventually of vanishing width) are indicated by the theory, yet this number is further limited by Eq. (8). There need to be channel walls of zero thickness between the lateral channels. Moreover, the value of ψ implicit in Eqs. (3) and (5) may not be easily obtainable (except in cases of symmetry).

While the unphysical perturbation $\mathbf{g}_m$ is not realizable, an approximation is clearly possible through the approach described. This is probably the first insight into the best configuration of lateral channels in cross-channel micromixers. It can be readily applied in geometries other than the paradigmatic situation shown in Fig. 1; all that needs to be done is to determine a Hamiltonian function for the base flow that conforms to the geometry and flow velocities relevant to the required device. The analysis technique described here can then be applied. It is hoped that this paper will stimulate the development of experimental devices to test the results.

[1] D. R. Meldrum and M. R. Holl, "Microscale bioanalytic systems," Science **297**, 1197 (2002).
[2] H. A. Stone and S. Kim, "Microfluidics: Basic issues, applications and challenges," AIChE J. **47**, 1250 (2001).
[3] D. D. Cunningham, "Fluidics and sample handling in clinical chemical analysis," Anal. Chim. Acta **429**, 1 (2001).
[4] T. H. Schulte, R. L. Bardell, and B. H. Weigl, "Microfluidic technologies in clinical diagnostics," Clin. Chim. Acta **321**, 1 (2002).
[5] B. H. Weigl, R. L. Bardell, and C. R. Cabrera, "Lab-on-a-chip for drug development," Adv. Drug Delivery Rev. **55**, 349 (2003).
[6] D. J. Beebe, G. A. Mensing, and G. M. Walker, "Physics and applications of microfluidics in biology," Annu. Rev. Biomed. Eng. **4**, 261 (2002).
[7] F. Bottausci, I. Mezić, C. D. Meinhart, and C. Cardonne, "Mixing in the shear superposition micromixer: Three dimensional analysis," Philos. Trans. R. Soc. London, Ser. A **362**, 1001 (2004).
[8] P. Taberling, M. Chabert, A. Dodge, C. Julien, and F. Okkels, "Chaotic mixing in cross-channel micromixers," Philos. Trans. R. Soc. London, Ser. A **362**, 987 (2004).
[9] A. Dodge, M. Jullien, Y.-K. Lee, X. Niu, F. Okkels, and P. Taberling, "An example of a chaotic micromixer: The cross-channel micromixer," C. R. Phys. **5**, 557 (2004).
[10] M. Volpert, C. D. Meinhart, I. Mezić, and M. Dahleh, "An actively controlled micromixer," in *Proceedings of ASME Mechanical Engineering International Congress and Exposition*, MEMS Vol. 1 (ASME, Nashville, TN, 1999), p. 463.
[11] A. D. Stroock, S. K. W. Dertinger, A. Ajdari, I. Mezić, H. A. Stone, and G. M. Whitesides, "Chaotic mixer for microchannels," Science **295**, 647 (2002).
[12] B. R. Noack, I. Mezić, G. Tadmor, and A. Banaszuk, "Optimal mixing in recirculation zones," Phys. Fluids **16**, 867 (2004).
[13] D. D'Alessandro, M. Dahleh, and I. Mezić, "Control of mixing in fluid flow: A maximum entropy approach," IEEE Trans. Autom. Control **44**, 1852 (1999).
[14] H. Aref, "The development of chaotic advection," Phys. Fluids **14**, 1315 (2002).

[15] A. Vikhansky, "Quantification of reactive mixing in laminar microflows," Phys. Fluids **16**, 4738 (2004).
[16] L.-H. Lu, K. S. Ryu, and C. Liu, "A magnetic microstirrer and array for microfluidic mixing," J. Microelectromech. Syst. **11**, 462 (2002).
[17] R. S. MacKay, J. D. Meiss, and I. C. Percival, "Transport in Hamiltonian systems," Physica D **13**, 55 (1984).
[18] T. H. Solomon, S. Tomas, and J. L. Warner, "Role of lobes in chaotic mixing of miscible and immiscible impurities," Phys. Rev. Lett. **77**, 2682 (1996).
[19] G. A. Voth, G. Haller, and J. P. Gollub, "Experimental measurements of stretching fields in fluid mixing," Phys. Rev. Lett. **88**, 254501 (2002).
[20] A. Vikhansky, "Control of stretching rate in time-periodic chaotic flows," Phys. Fluids **14**, 2752 (2002).
[21] M. D. Finn, S. M. Cox, and H. M. Byrne, "Mixing measures for a two-dimensional chaotic Stokes flow," J. Eng. Math. **48**, 129 (2004).
[22] S. Balasuriya, "Optimal perturbation for enhanced chaotic transport," Physica D **202**, 155 (2005).
[23] S. Balasuriya, "Direct chaotic flux quantification in perturbed planar flows: General time-periodicity," SIAM J. Appl. Dyn. Syst. **4**, 282 (2005).
[24] V. Rom-Kedar, A. Leonard, and S. Wiggins, "An analytical study of transport, mixing and chaos in an unsteady vortical flow," J. Fluid Mech. **214**, 347 (1990).
[25] S. Wiggins, *Chaotic Transport in Dynamical Systems* (Springer, New York, 1992).
[26] J. Guckenheimer and P. Holmes, *Nonlinear Oscillations, Dynamical Systems, and Bifurcations of Vector Fields* (Springer, New York, 1983).
[27] V. Rom-Kedar and A. C. Poje, "Universal properties of chaotic transport in the presence of diffusion," Phys. Fluids **11**, 2044 (1999).
[28] S. Chandrasekhar, *Hydrodynamics and Hydrodynamic Stability* (Dover, New York, 1961).
[29] T. Ahn and S. Kim, "Separatrix-map analysis of chaotic transport in planar periodic vortical flows," Phys. Rev. E **49**, 2900 (1994).
[30] S. S. Abdullaev, "Structure of motion near saddle points and chaotic transport in Hamiltonian systems," Phys. Rev. E **62**, 3508 (2000).
[31] B. I. Shraiman, "Diffusive transport in a Rayleigh-Bénard convection cell," Phys. Rev. A **36**, 261 (1987).
[32] T. H. Solomon and J. P. Gollub, "Chaotic particle transport in time-dependent Rayleigh-Bénard convection," Phys. Rev. A **38**, 6280 (1988).